

FMCW Chirp Diversity for Mutual Interference Mitigation in Short-range Automotive Radars under Realistic Traffic Model

Md Anowar Hossain, Ibrahim Elshafiey, and Abdulhameed Al-Sanie

Electrical Engineering Department
King Saud University, 11421, Riyadh, Saudi Arabia
ahossain@ksu.edu.sa, ishafiey@ksu.edu.sa, sanie@ksu.edu.sa

Abstract — With the worldwide harmonized frequency allocation for automotive radars and increasing rate of modern vehicles equipped with radar systems, mutual interference among automotive radars is becoming a key problem. This paper presents a novel approach for mutual interference mitigation based on diverse waveform design by imposing time and frequency diversity to frequency modulated continuous wave (FMCW) chirp signal considering 79 GHz short-range automotive radar. Performance of the proposed waveform in terms of auto-correlation and cross-correlation has been investigated using software-defined radio (SDR) transceiver and measurement results are provided. The system concept is validated by developing an automotive radar channel model considering a realistic 3D road traffic scenario using a ray-tracing tool. Theoretical analysis and simulation examples of different mutual interference scenarios in an automotive environment are provided to evaluate the effectiveness of the proposed method. Results show that the proposed waveform is able to detect the targets of interest successfully while mitigating the false targets in mutual interference environments.

Index Terms — Automotive radar, FMCW chirp, mutual interference, waveform diversity.

I. INTRODUCTION

Improving traffic efficiency and reducing road accidents are challenging tasks in most regions of the world. Traffic congestions and road accidents have been increasing, especially in urban roads and highways due to population growth as well as increasing numbers of vehicles and economic activities. Although the amount of road accidents was reduced during the last decade by introducing both traffic law enforcement and passive safety means (seatbelt, airbag), the number of accidents has remained uniform because of the increasing number of vehicles.

Recent advances in microelectronic technology provides high-performance and low-cost radar sensors

suitable for automotive applications [1-3]. Thus, radar based active safety functions are being integrated into all classes of vehicles to further reduce the amount of road accidents, as they are robust against weather conditions and other environmental hazards. This will result in a high density distributed automotive radar network operating simultaneously in a close proximity, which introduces mutual interference among multiple automotive radars due to shared spectrum usage, lack of coordination among multiple radars and road traffic situation [4]. Moreover, the automotive industry and research community is currently developing vehicular communication based on IEEE 802.11p dedicated short range communication (DSRC) band at 5.9 GHz [5]. The estimated position and velocity information using automotive radar can be exchanged among the neighbor vehicles on the road to implement cooperative driving for optimizing traffic efficiency. This requires highly reliable position information of surrounding vehicles from automotive radar equipped vehicles.

II. LITERATURE REVIEW

Mutual interference in automotive radars has not been investigated much yet apart from a few efforts. Theoretical background of next generation automotive radar is analyzed in [6]. The impact of mutual interference and measurement possibilities to test and verify mitigation techniques in arbitrary RF environments with norm interferers are presented in detail. Modelling of automotive radar interference based on stochastic geometry methods is presented in [7]. The developed model has further been used to estimate the detection probability of target vehicles. Discussion of the operating range of FMCW radars in presence of interference is presented in [8]. The influence of different kinds of interference on the spectrum of a FMCW radar is shown based on measurements and simulations. However, the conventional FMCW waveform with constant slope introduces false targets due to mutual interference when multiple radars are being operated simultaneously. A modified LFM CW waveform based on the modulation

of sweep slope is proposed in [9] to mitigate the mutual interference. However, it was assumed that the pattern of sweep slope is orthogonal among multiple radars to successfully mitigate the false targets. In practice, perfect orthogonal waveforms cannot be implemented in automotive radar networks due to the lack of coordination among radars. Waveform generation for automotive radar with multiple frequency shift keying (MFSK) is presented in [10]. MFSK based automotive radars exhibit excellent speed resolution, but due to the poor range resolution, it is difficult to discriminate between two target vehicles with identical relative speed. Furthermore, target vehicles with the same speed as the radar cannot be detected at all [11]. Noise radar technology as an interference prevention method is provided in [12]. Unfortunately, this type of radar exhibits several drawbacks such as complexity in signal processing and near-far problems. Furthermore, the required computational power is very high and it is difficult to apply the noise radar signal processing in real time for high bandwidth radars. Waveform generation for automotive radar based on the spread spectrum technique for mutual interference mitigation is proposed in [13]. Spread spectrum provides a measure of immunity to multipath interference and multiple access capability, making it ideal for radar applications. However, it requires extremely fast circuitry to generate the chip sequence, because the processing gain is determined by the ratio of the chip rate to the bit rate. In addition, spread spectrum systems often require adaptive power control techniques to overcome the near-far problem.

Most of these prior research works consider the automotive radar environments as simple stochastic channel models based on the statistical properties of the surrounding environment of vehicles. Such models do not exhibit the actual evaluation of automotive radar applications because static objects such as buildings and foliage, and mutual interference from the radar of surrounding vehicles exhibit significant impact on automotive radar performance. For effective performance evaluation of an automotive radar system, realistic traffic environment and wave propagation models should be considered. That helps in evaluating system performance efficiently. Field measurement is also a possible solution, but it is expensive and provides no repeatability.

Based on this background, simulation of automotive radars under realistic environment is considered, and advanced waveform design technique is proposed in this paper to mitigate false targets due to mutual interference. To evaluate the performance of automotive radar in realistic environments, we have developed a ray-tracing model that includes every domain involved, such as advanced waveform design, transmitter and receiver frontends, and realistic 3D road traffic environment.

The remaining parts of the paper are organized as follows. Section III describes the mutual interference

scenarios in automotive environments. The proposed FMCW waveform design technique is provided in Section IV. Experimental validation to evaluate the effectiveness of proposed waveform is provided in Section V. Section VI describes the developed ray-tracing simulation model considering realistic 3D road traffic environment. Section VII presents the post processing and target detection with thorough analysis of results and discussions. Final conclusions are given in Section VIII.

III. MUTUAL INTERFERENCE IN AUTOMOTIVE RADARS

Currently, only small amount of vehicles are equipped with radar sensors. Thus, in most of the cases, the scattered signals of other radars will be obstructed by further vehicles without radars in between the radar equipped vehicle (V1) and the second automotive radar (V2) as shown in Fig. 1. Usually, these unwanted indirect signals exhibit a very low energy that contributes to the noise floor. Thus, thermal noise, unwanted returns coming from the road-surface or various objects adjacent to the road (buildings and foliage) are the main source of interference in current situation.

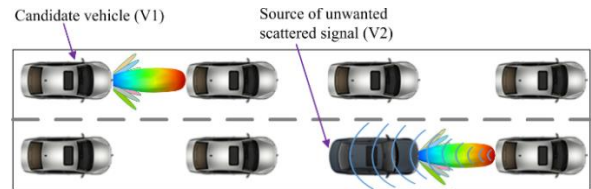


Fig. 1. Mutual interference due to scattered signals from another automotive radar.

When more vehicles will be equipped with radar sensors in near future, the indirect reflections due to the radars of neighbor vehicles will be almost the same order of magnitude as the reflected signal of the candidate vehicle's own radar. For example, indirect signals can be received by two candidate vehicles with forward looking radars moving along next to each other and a target vehicle is at some distance ahead as shown in Fig. 2.

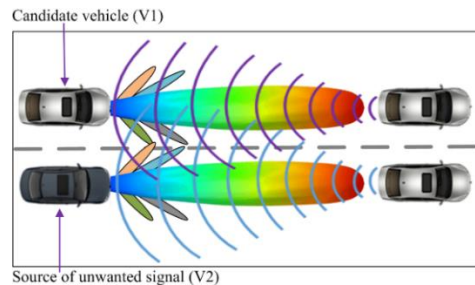


Fig. 2. Mutual interference due to indirect signals from another automotive radar.

A direct input of unwanted signal into the radar equipped vehicle can occur when the candidate vehicle is illuminated by the radar of another vehicle. For example, two vehicles V1 and V2 equipped with forward looking radars can be illuminated by each other as shown in Fig. 3. This situation can occur on the roads where adjacent lanes have traffic travelling in opposite directions. The direct reception of transmitted signal from radars of neighbor vehicles will be higher magnitude than the reflected signal of the candidate vehicle's own radar.

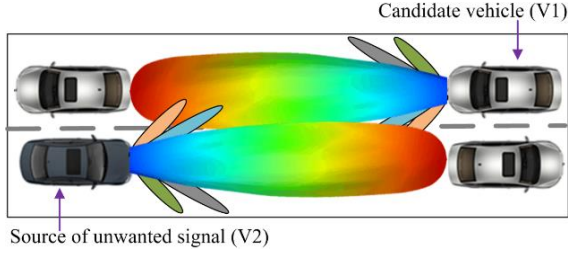


Fig. 3. Mutual interference due to direct signals between automotive radars.

For automotive radar under mutual interference, the radar equipped with the candidate vehicle will receive signals from other radars due to overlapping of mainlobes and side-lobes of antenna beams. Thus, the received signals for n th radar can be given as:

$$\Psi_{rx,n}(t) = \sum_{m=1}^M h_{m,n}(t) \Psi_{tx,m}(t - \tau_{m,n}) + \eta(t), \quad (1)$$

where, $m \in [1, 2, \dots, M]$ and $n \in [1, 2, \dots, N]$ are the number of transmitting and receiving radars, $\Psi_{tx,m}(t)$ is the transmitted waveform of m th radar, $h_{m,n}(t)$ is the channel coefficient associated with m th transmitting and n th receiving radar, $\tau_{m,n}$ is the signal propagation time related to m th transmitting antenna to n th receiving antenna and $\eta(t)$ is the AWGN.

If we perform matched filtering (dechirping) to extract the signal associated with candidate radar considering $m=1$, then equation (1) can be modified as:

$$\Psi_{MF,n}(t) = \Psi_{rx,n}(t) \otimes \Psi_{tx,1}^*(-t), \quad (2)$$

$$\begin{aligned} \Psi_{MF,n}(t) = & h_{1,n}(t) \Psi_{tx,1}(t - \tau_{1,n}) \otimes \Psi_{tx,1}^*(-t) \\ & + \sum_{m=2}^M h_{m,n}(t) \Psi_{tx,m}(t - \\ & \tau_{m,n}) \otimes \Psi_{tx,1}^*(-t) + \eta(t) \otimes \Psi_{tx,1}^*(-t), \end{aligned} \quad (3)$$

where, \otimes denotes the convolution operator, the first term in equation (3) is the desired MF output, the second term is the mutual interference that is required to be mitigated. The third term is the system noise. The term related to mutual interference can be completely mitigated if the waveforms transmitted from multiple automotive radars are orthogonal to each other and can be given as:

$$\sum_{m=2}^M h_{m,n}(t) \Psi_{tx,m}(t - \tau_{m,n}) \otimes \Psi_{tx,1}^*(-t) = 0. \quad (4)$$

However, perfect orthogonal waveforms cannot be

implemented in automotive radar network due to use of shared spectrum and the lack of coordination among radars resulting from the absence of centralized control and resource allocation unit. Thus, advanced waveform design and signal processing methods need to be incorporated to mitigate the automotive radar interference issues. If the automotive radar transmits a unique chirp at each sweep i.e. different slope at each sweep based on the advanced waveform design technique with time and frequency diversity, then matched filtering output of the candidate radar exhibits strong auto-correlation with its own transmitted signal and weaker cross-correlation properties with reflected or transmitted signals from other neighbor radars which in turns improve the detection of target vehicles and mitigate the false targets due to mutual interferences.

IV. ADVANCED WAVEFORM DESIGN

In general, automotive radar systems adopt FMCW waveform due to the possibilities of target estimation through runtime measurements. Compared to pulsed radars, FMCW radars require less power and exhibit reduced size and cost. The FMCW chirp signal can be given as:

$$\Psi_{tx}(t) = \cos \left[2\pi t \left(f_0 + \frac{\beta t}{2} \right) \right], \quad (5)$$

where β denotes the sweep slope and is given as:

$$\beta = \frac{f_1 - f_0}{T} = \frac{B}{T}, \quad (6)$$

where f_0 and f_1 are the starting frequency and final frequency respectively. The terms B and T are sweep bandwidth and sweep time respectively. The sweep time T can be computed based on the time needed for the signal to travel the unambiguous maximum range and is given as:

$$T = \alpha \frac{2R_{max}}{c}, \quad (7)$$

where α denotes the slope factor, R_{max} is the unambiguous maximum range and c is the speed of light. The sweep bandwidth is related to range resolution (ΔR) and can be given as:

$$B = \frac{c}{2\Delta R}. \quad (8)$$

In general, for an FMCW radar system, the slope factor is considered as at least 5 to 6 times the round trip time. Thus, for reliable target detection in mutual interference environments, we can obtain a unique slope (β) at each sweep by modulating both sweep time and sweep bandwidth. The modulation in sweep time can be obtained considering variations in sweep factor (α) for a given maximum unambiguous range. The modulation in sweep bandwidth can be selected based on the required range resolution.

We consider FMCW chirp signal with triangular sweep that sweeps-up with a slope of (B/T) and sweeps-down with a slope of $(-B/T)$. B is the sweep bandwidth, and T is the sweep time. Figure 4 (a) shows the

spectrogram representation of 16 sweeps based on the conventional triangular FMCW chirp signal with constant slope for all sweeps and Fig. 4 (b) shows the proposed FMCW chirp with random slope considering both time and frequency diversity at different triangular sweeps.

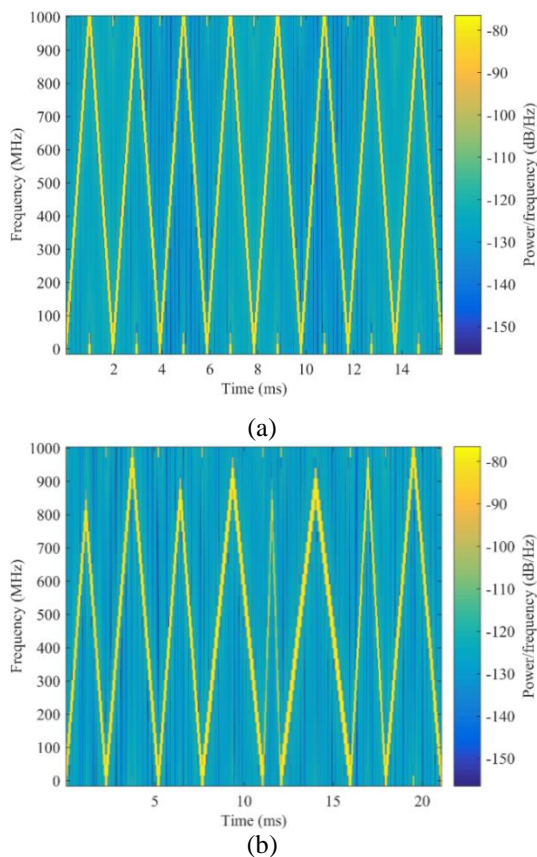


Fig. 4. Spectrogram representation of FMCW signal: (a) conventional triangular sweep, and (b) proposed triangular sweep with time and frequency diversity.

V. EXPERIMENTAL VALIDATION

It is important to ensure that the chirp signal of one radar must pose lower cross-correlation to that of another radar. Performance of the proposed waveform can be investigated by analyzing the auto-correlation and cross-correlation of the chirp signals. Hardware measurements of the proposed waveform in terms of auto-correlation and cross-correlation are conducted to assess the efficiency of the proposed waveform in mutual interference environment. Different from the 79 GHz band considered in ray-tracing simulation, an existing transceiver system from National Instrument (NI) with LabVIEW is adopted for measurements. Two NI 5791R RF transceiver adapter modules with built in FPGA are connected with NI 1085 chassis. The NI PXIe-1085

18-slot chassis features a high-bandwidth, all-hybrid backplane to meet a wide range of high-performance test and measurement application needs. The NI 5791R is an RF transceiver adapter module with 120 MHz bandwidth designed to work in conjunction with NI 7975 FlexRIO FPGA module. The NI 5791 features two channel analog-to-digital converter (ADC) and digital-to-analog converter (DAC) with 130 MS/s. It can upconvert and downconvert RF signals ranging from 200 MHz to 4.4 GHz. The hardware setup is shown in Fig. 5. We connect two transceivers at slot 6 and slot 12 of the chassis. A LabVIEW model has been developed to generate, transmit, and receive the chirp waveform. The model can also compute the correlation between transmitted and received signal. The model includes the flexibility of changing system parameters such as carrier frequency, starting and final frequency for chirp generation and output power at the transmitter. The auto-correlation and cross-correlation results have been obtained as follows:

- For auto-correlation, FMCW chirp has been generated and transmitted considering the carrier frequency of 4 GHz and sweep bandwidth of 100 MHz. The correlation between received signal and baseband transmitted signal was obtained.
- For cross-correlation, FMCW chirp has been generated and transmitted considering the carrier frequency of 3.75 GHz and sweep bandwidth of 120 MHz. The correlation between received signal and baseband transmitted signal in part (a) was obtained.

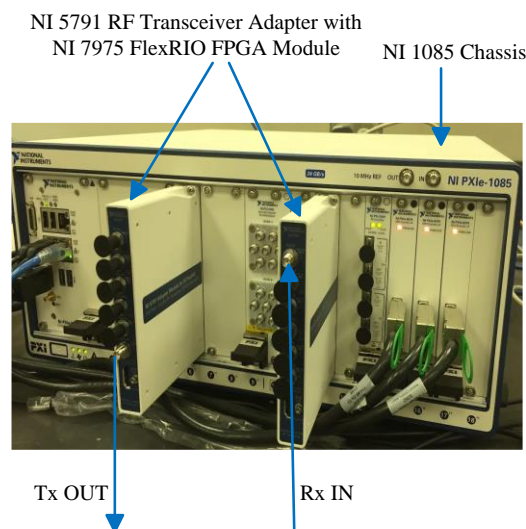


Fig. 5. NI 5791 adapter in conjunction with NI 7975 connected to NI 1085 chassis.

The auto-correlation and cross-correlation results are shown in Fig. 6 and Fig. 7 respectively. It is observed that the simulated and measured correlation results are in good agreement.

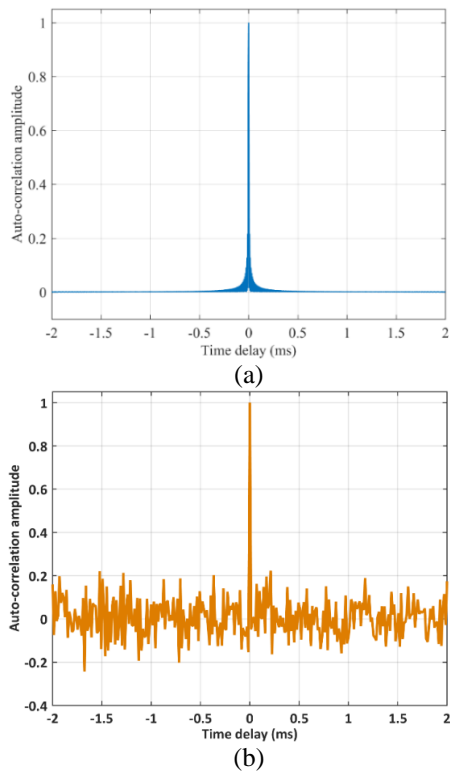


Fig. 6. Auto-correlation results of the proposed FMCW chirp. (a) Simulated and (b) measured.

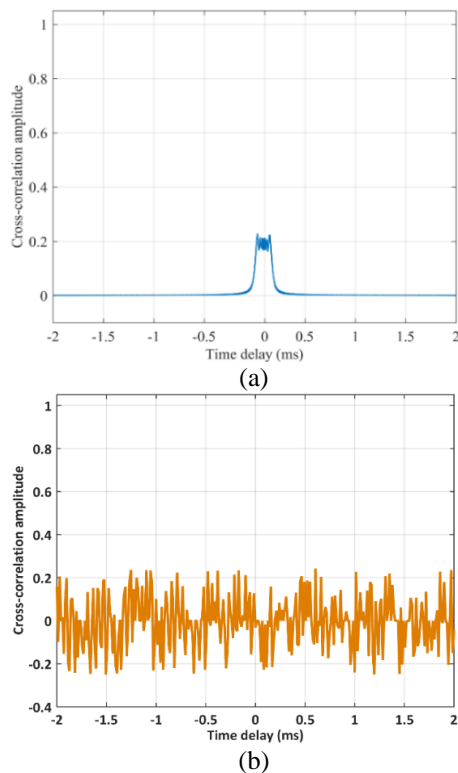


Fig. 7. Cross-correlation results of the proposed FMCW chirp. (a) Simulated and (b) measured.

For an effective comparison, the normalized auto-correlation and cross-correlation amplitude are provided with the same scale. It is observed that the proposed diverse FMCW chirp signal exhibits strong correlation characteristics, a sharp autocorrelation peak with same chirp, and lower cross-correlation with two chirp with different sweep slope considering time and frequency diversity. Thus, although the neighbor automotive radars contribute to the received signals, the received signals corresponding to transmitted chirp can be extracted efficiently in the correlation process.

VI. REALISTIC TRAFFIC SCENARIO AND WAVE PROPAGATION MODEL

Realistic and efficient modeling of the signal propagation scenario is the basis for successful evaluation of automotive radar applications. Physical characteristics of the received signal directly affect the upper layers in discriminating the range, angle and speed of the target vehicles. Realistic modeling of automotive radar channels requires the consideration of complex environments such as static objects (road terrain, buildings and foliage) and moving objects (neighbor vehicles on the road). The time-variant nature of the propagation channel for automotive radar is not only affected by the motion of the vehicles, but also by surrounding vehicles and objects adjacent to the road. Thus, to develop a realistic automotive radar channel, proper consideration of the scenario is necessary.

Figure 8 shows the automotive radar channel model that we developed using Wireless Insite ray-tracing tool [14]. To develop a realistic channel, the model randomly considers objects such as buildings of different size and shape, road terrain and tree foliage adjacent to the road. The model also includes vehicles equipped with radar unit and vehicles without radar unit as targets. These objects are designed individually and characterized with relevant material properties such as metal, glass etc. as shown in Table 1. Finally, all objects are integrated into a complete automotive radar channel model. This combination yields a virtual automotive radar environment and allows for the investigation of system performance in realistic approach.

Table 1: Considered object characterization

Object	Material
Body of vehicle	Metal
Vehicle mirrors	Glass
Wheels	Rubber
Front and rear bumpers	Plastic
Road terrain	Asphalt
Buildings	Brick
Tree foliage	Wood and leaf

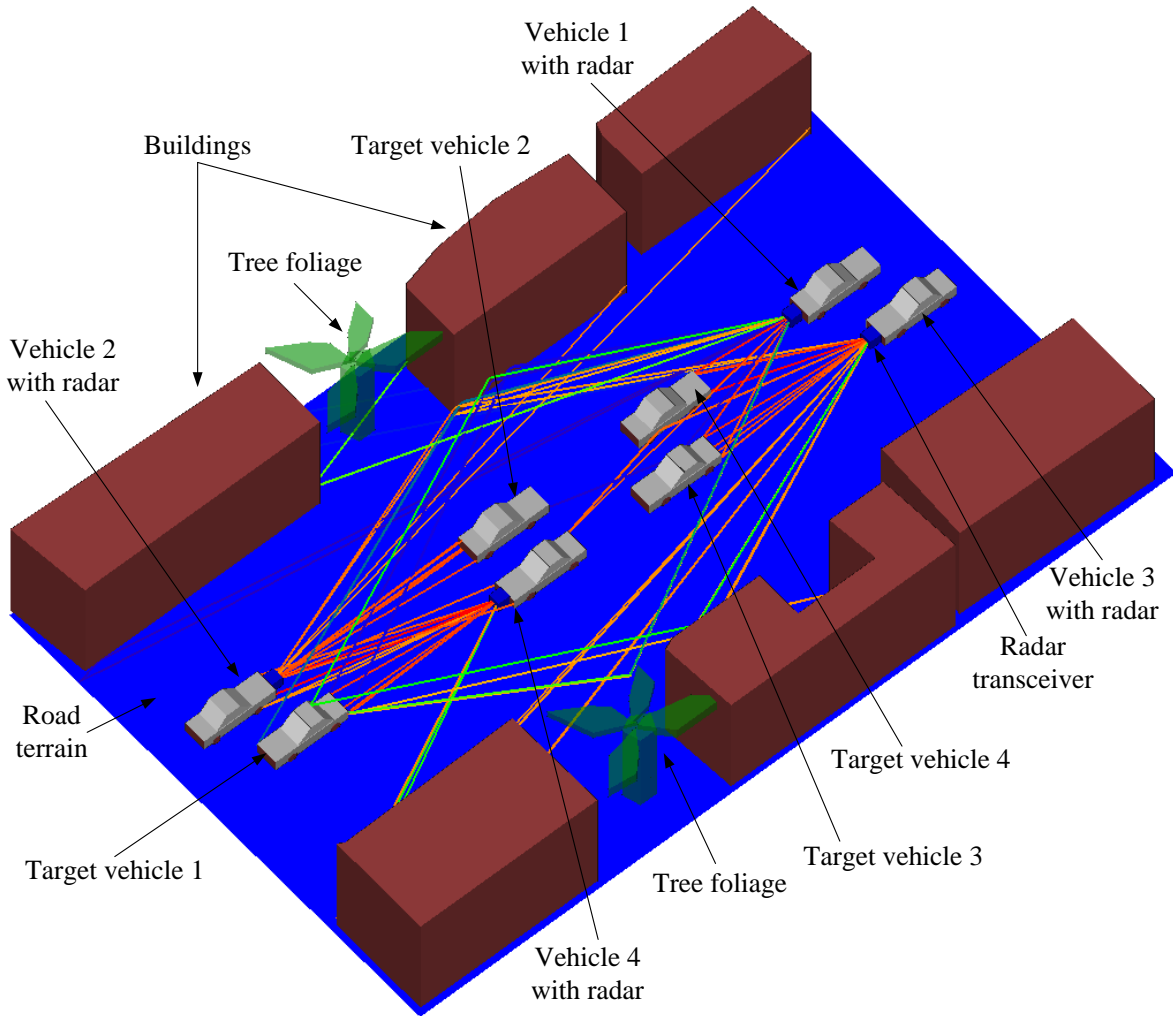


Fig. 8. Developed 3D automotive radar channel model using Wireless Insite ray-tracing tool.

Simulated data of the proposed FMCW waveform (time stamp and samples) are imported into the ray-tracing simulator as user defined waveform. The phased array and transceiver front end are parameterized in ray-tracing tool. The phased-array is configured as 4-element uniform linear array (ULA) considering directional antenna with 3-dB beamwidth of $\pm 80^\circ$ and $\pm 10^\circ$ in azimuth and elevation respectively. Table 2 shows the parameters used in signal generation and transmitter-receiver front end. The received signals are obtained by shooting rays from the transmitters and propagating them through the defined geometry of the developed channel model. These rays interact with geometrical features and make their way to receiver locations. Ray interactions include reflections from feature faces, diffractions around feature edges, and transmissions through features faces. All possible reflections of the transmit signal towards the position of the receiver are generated considering a realistic 3D traffic environment

and wave propagation model developed using Wireless Insite ray-tracing tool. For every propagation path the time-domain received signal are calculated considering the related dielectric material properties of the reflecting object. Finally, post processing of the received signal has been performed to detect the range, angle and speed of the target vehicles.

Table 2: Simulation parameters

Parameter	Value
Operating frequency	79 GHz
Maximum target range	30 m
Sweep time	1-2 ms
Sweep bandwidth	800-1000 MHz
Transmit power	10 dBm
Transmit gain	36 dB
Receive gain	42 dB

VII. RESULTS AND DISCUSSION

We have considered a scenario that includes eight vehicles where four vehicles are equipped with automotive radars. We consider that radar equipped vehicle 1, 2 and target vehicle 2, 4 are in lane 1 respectively and moving toward right direction while radar equipped vehicle 3, 4 and target vehicle 1, 3 are in lane 2 and moving towards left direction as shown in Fig. 8. All possible reflections of the transmit signal towards the position of the receiver are generated using developed model in Wireless Insite ray-tracing tool. For every propagation path the time-domain received signal are calculated considering the related dielectric material properties of the reflecting object.

Dechirping is performed by mixing the output signal of the receiver front end with the reference signal. Beamforming is then applied considering a phase-shift beamformer to enhance the detection of signals by coherently summing signals across elements of arrays. The beamforming outputs are buffered for each sweep. The first step in the signal processing step is range estimation. Once the range of the targets are estimated, the data in the corresponding range bins are used to estimate the speed and angle of the same target. For range detection, the buffered signal for each sweep are converted to frequency domain. The beat frequencies of dechirped signals are converted to corresponding range and the target range is estimated. For triangular FMCW chirp, the up-sweep and down-sweep have separate beat frequencies. The difference between frequency of the transmitted and received signals during up-sweep and down-sweep frequency ramp is called the up-sweep beat frequency (f_{bu}) and down-sweep beat frequency (f_{bd}) respectively. The range estimation can be given as [15]:

$$R = \frac{cT}{4B} \cdot \frac{(f_{bu} + f_{bd})}{2}, \quad (9)$$

where B and T are the sweep bandwidth and sweep time respectively. For speed estimation, the Range-Doppler response is computed by converting dechirp data into frequency domain. The Doppler domain data is then converted to speed to determine the relative speed between radar and the target vehicles. The relative velocity of the target can be given as:

$$V_r = \frac{\lambda}{2} \cdot \frac{(f_{bd} - f_{bu})}{2}. \quad (10)$$

Where λ denotes the wavelength. The terms f_{bu} and f_{bd} are the up-sweep and down-sweep beat frequencies respectively. The angle estimation of target vehicles can be performed by converting dechirp output in frequency domain and applying root MUSIC algorithm [16].

From the ray-tracing output, we obtain the received signal for all Tx-Rx combinations. Based on the ray-analysis as shown in Fig. 8, it is observed that each radar receives the reflected signals associated

with its own transmission as well as the reflected or direct signal from other radars. Let us investigate the target detection performance of automotive radar based on the conventional FMCW waveform and the proposed waveform with time and frequency diversity under different scenarios as follows.

A. Ideal scenario without mutual interference

Let us assume an ideal scenario, i.e., without any mutual interference. We consider the conventional FMCW waveform with the same slope as transmitted signals from radar equipped vehicle 1 and 2 as shown in Fig. 8. The reflected signal associated only with the transmitted signal from the candidate radar are considered in the dechirping process. Figure 9 (a) shows that radar equipped on rear bumper of vehicle 1 estimates the range of target vehicles 3 and 4 accurately at about 9.15 and 6.5 meters respectively. Figure 9 (b) shows the radar equipped vehicle 2 estimates the range of target vehicle 2 and radar equipped vehicle 4 accurately at about 12.6 and 13.65 meters respectively. Thus, it is observed that the range of target vehicles is estimated accurately with negligible ambiguities or unwanted peaks with lower values from roadside buildings and road terrain.

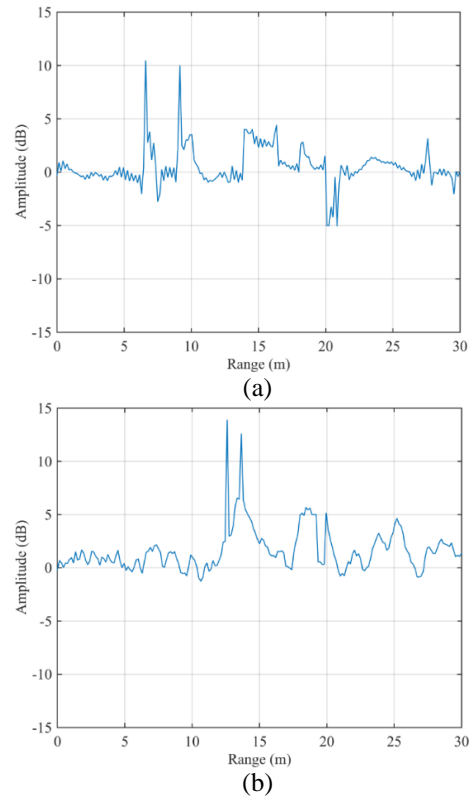


Fig. 9. Estimated range of target vehicles (a) target vehicles 3 and 4 are detected at radar equipped vehicle 1 and (b) target vehicle 2 and radar equipped vehicle 4 are detected at radar equipped vehicle 2.

B. Mutual interference due to indirect signal

Let us consider the mutual interference of indirect reflected signals due to the transmitted signal from other radars as shown in Fig. 2. In this scenario, radar equipped vehicles 1 and 3 are transmitting conventional FMCW waveform with constant slope in same directions to the target vehicles simultaneously as shown in Fig. 8. Thus, both radars will receive the reflected signal from the target vehicles due to the transmission of other radar. Let us consider the target detection in radar equipped vehicle 1 including the indirect interference from radar equipped vehicle 3. Figure 10 (a) shows the range estimation results of radar equipped vehicle 1. It is observed that four targets are detected where two false targets are introduced due to indirect mutual interference from radar equipped vehicle 3.

Let us investigate the same scenario by transmitting two different FMCW waveforms from radar equipped vehicles 1 and 3 with time and frequency diversity at each sweep considering the proposed waveform design technique. The dechirping operations for this case can be given as:

$$\Psi_{MF,n}(t) = \Psi_{rx,n}(t) \otimes \Psi_{tx,n}^*(-t), \quad (11)$$

where $\Psi_{rx,n}(t)$ and $\Psi_{tx,n}(t)$ are the received signal and transmitted signal associated with n th radar respectively. Figure 10 (b) shows the range estimation results of radar equipped vehicle 1 based on the proposed FMCW waveform. It is observed that the two target vehicles are detected successfully and false targets due to indirect interference from radar equipped vehicle 3 are mitigated.

C. Mutual interference due to direct signal

Let us consider the mutual interference due to the direct signal transmitted from other radars as shown in Fig. 3. In this scenario, radar equipped vehicles 2 and 4 as shown in Fig. 8 are in opposite directions and transmitting conventional FMCW waveforms with same slope simultaneously. Thus, both radars will receive the delayed version of the transmitted signal directly from other radar. Let us consider the target detection in radar equipped vehicle 2 including the direct interference from radar equipped vehicle 4.

Figure 11 (a) shows the range estimation results of radar equipped vehicle 2. It is observed that three targets are detected where one false target is introduced at about 6.6 meters due to the direct reception of delayed version of the transmitted signal from radar equipped vehicle 4. It is also observed that the amplitude of the false target is higher than the actual target because of the direct reception of the transmitted signal.

Let us investigate the same scenario by transmitting two different FMCW waveform in radar

equipped vehicles 2 and 4 with time and frequency diversity at each sweep considering the proposed waveform design technique. Figure 11 (b) shows the range estimation results of radar equipped vehicle 2 based on the proposed FMCW waveform. It is observed that the two vehicles (target vehicle 2 and radar equipped vehicle 4) are detected successfully at 12.6 meters and 13.65 meters respectively and false target at 6.6 meters is mitigated.

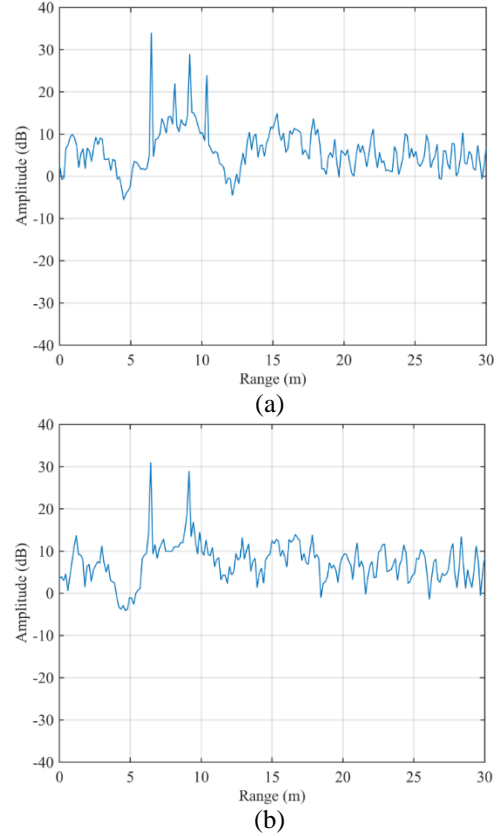


Fig. 10. Estimated range of target vehicles at radar equipped vehicle 1: (a) four target vehicles are detected including two false targets due to indirect mutual interference from radar equipped vehicle 3, and (b) two target vehicles are detected without false targets.

To evaluate the effectiveness of the proposed waveform in multi-target scenarios, the ray-tracing model is modified for varying number of target vehicles at different locations of the road terrain. The received signals for each scenario are processed to estimate the range, angle and speed of the target vehicles. For target detection, we consider adaptive decision threshold based on the mean of the matched filtering output, which is given as:

$$\delta = E\{\Psi_{MF,n}(t)\}, \quad (12)$$

where $E\{\cdot\}$ denotes the average of the dechirping output. For an effective analysis, the probability of target detection as well as root mean-squared errors (RMSE) between actual and estimated range, angle and speed of the target vehicles are obtained as:

$$RMSE = \sqrt{\frac{1}{N} \sum_{n=1}^N [\phi - \hat{\phi}]^2}, \quad (13)$$

where ϕ and $\hat{\phi}$ are the actual and estimated values of range, angle and speed of the target vehicles.

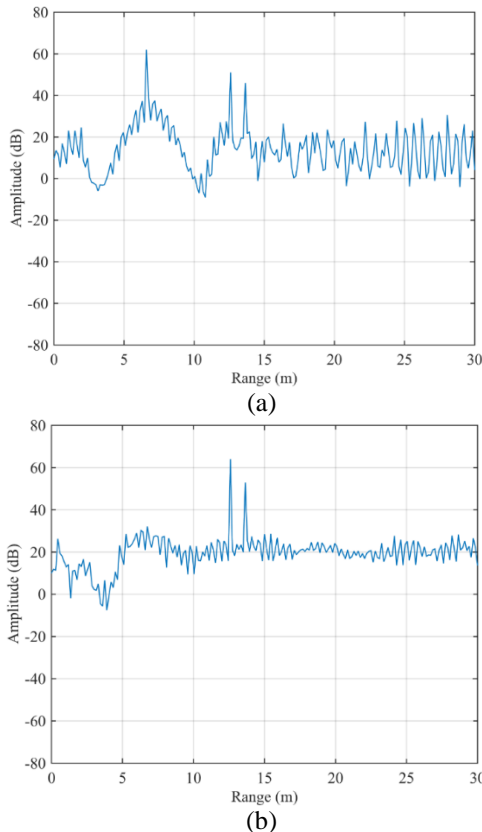


Fig. 11. Estimated range of target vehicles at radar equipped vehicle 2: (a) three target vehicles are detected including one false target due to direct mutual interference from radar equipped vehicle 4, and (b) two target vehicles are detected without false target.

The probability of detection for varying numbers of target vehicles is shown in Fig. 12, where the probability of detection can be defined as the ratio of the number of detected real targets to the number of total real targets. It is observed that the proposed waveform outperforms the conventional FMCW waveform and exhibits higher probability of target detection. Figure 13 shows the RMSE of range, angle and speed for varying number of target vehicles. It is observed that RMSE increases with the number of target vehicles increases. The proposed waveform

exhibits multi-target detection with range accuracy of about 0.13 m, angle and speed accuracy of about 0.12° and 0.1 km/h considering 10 target vehicles.

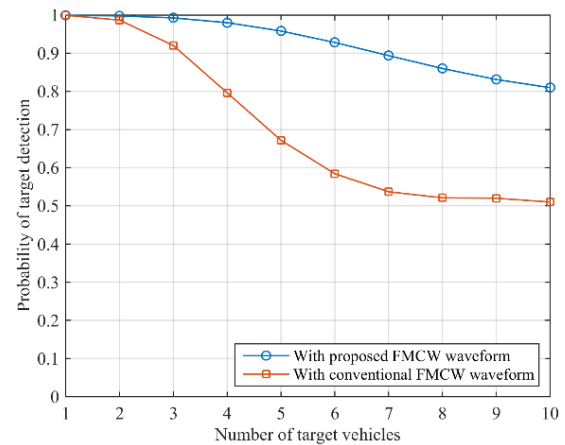


Fig. 12. Detection probability for varying number of target vehicles.

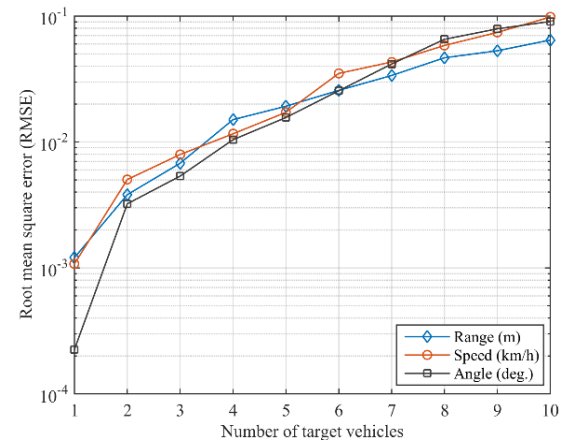


Fig. 13. Root mean squared error (RMSE) for varying number of target vehicles.

VIII. CONCLUSION

Advanced waveform design technique is proposed for multi-target detection and mutual interference mitigation in short-range automotive radars. Ray-tracing model is developed that allows for investigating the entire signal flow considering the wave propagation in a realistic road traffic scenario. Performance of the proposed waveform in different mutual interference scenarios has been presented. The thorough analysis of the proposed system concept has been investigated in terms of detection accuracy and probability of detection. However, there are many additional aspects that can be investigated with the developed model, e.g., the performance investigation of different beamforming techniques and influence of various array configurations can be assessed under

realistic conditions. Hence, the developed realistic model can be regarded a comprehensive solution for the virtual performance evaluation of automotive radar concepts.

ACKNOWLEDGMENT

This work is supported by the Deanship of Scientific Research and Research Center at the College of Engineering, King Saud University, Riyadh, Saudi Arabia.

REFERENCES

- [1] B. H. Ku, P. Schmalenberg, O. Inac, O. D. Gurbuz, J. S. Lee, K. Shiozaki, and G. M. Rebeiz, "A 77-81 GHz 16-element phased-array receiver with $\pm 50^\circ$ beam scanning for advanced automotive radars," *IEEE Trans. on Microwave Theory and Techniques*, vol. 62, pp. 2823-2832, 2014.
- [2] N. Sönmez, F. Tokan, and N. Türker Tokan, "Double lens antennas in millimeter-wave automotive radar sensors," *Applied Computational Electromagnetics Society (ACES)*, vol. 32, no. 10, pp. 901-907, 2017.
- [3] V. Jain, F. Tzeng, L. Zhou, and P. Heydari, "A single-chip dual-band 77-81 GHz BiCMOS transceiver for automotive radars," *IEEE Journal of Solid-State Circuits*, vol. 44, pp. 3469-3485, 2009.
- [4] G. Brooker, "Mutual interference of millimeter-wave radar systems," *IEEE Trans. on Electromagnetic Compatibility*, vol. 49, pp. 170-181, 2007.
- [5] Y. Han, E. Ekici, H. Kremo, and O. Altintas, "Automotive radar and communications sharing of the 79-GHz band," *ACM Int. Workshop on Smart, Autonomous, and Connected Vehicular Systems and Services*, pp. 6-13, 2016.
- [6] S. Heuel, "Automotive radar sensors must address interference issues," *Microwave Journal*, vol. 59, pp. 22-36, 2016.
- [7] A. Al-Hourani, R. J. Evans, S. Kandeepan, B. Moran, and H. Eltom, "Stochastic geometry methods for modeling automotive radar interference," *IEEE Trans. on Intelligent Transportation Systems*, vol. 19, no. 2, pp. 333-344, 2018.
- [8] T. Schipper, M. Harter, T. Mahler, O. Kern, and T. Zwick, "Discussion of the operating range of frequency modulated radars in the presence of interference," *Int. Journal of Microwave and Wireless Technologies*, vol. 6, pp. 371-378, 2014.
- [9] Y. Kim, "Identification of FMCW radar in mutual interference environments using frequency ramp modulation," *European Conf. on Antennas and Propagation (EuCAP)*, pp. 1-3, 2016.
- [10] Q. Nguyen, M. Park, Y. Kim, and F. Bien, "77 GHz waveform generator with multiple frequency shift keying modulation for multi-target detection automotive radar applications," *Electronics Letters*, vol. 51, pp. 595-596, 2015.
- [11] C. Kärnfelt, A. Péden, A. Bazzi, G. E. H. Shhadé, M. Abbas, and T. Chonavel, "77 GHz ACC radar simulation platform," *Int. Conf. on Intelligent Transport Systems Telecommunications (ITST)*, pp. 209-214, 2009.
- [12] G. Galati and G. Pavan, "Noise radar technology as an interference prevention method," *Journal of Electrical and Computer Engineering*, vol. 2013, p. 4, 2013.
- [13] B. Kim and J. Lee, "Mutual interference-resilient vehicular spread spectrum radar using ZCZ code," *IEMEK Journal of Embedded Systems and Applications*, vol. 11, pp. 29-37, 2016.
- [14] Remcom. Wireless InSite. Available at: <http://www.remcom.com/wireless-insite>
- [15] S. Kim, I. Paek, and M. Ka, "Simulation and test results of triangular fast ramp FMCW waveform," *IEEE Radar Conf.*, pp. 1-4, 2013.
- [16] H. L. Van Trees, "Optimum array processing, part IV of detection, estimation, and modulation theory," EISBN: 0-471-09390-4, pp. 362-382, 2002.



Md Anowar Hossain received his B.S. degree in Computer and Communication Engineering from International Islamic University Chittagong. He obtained his M.S. and Ph.D. degrees in Electrical Engineering from King Saud University. He is currently

working as a Researcher in the Electrical Engineering Department, King Saud University. His research interests include radar signal processing, automotive radar, intelligent transportation system (ITS), cooperative driving, vehicular communication, and software-defined radio (SDR) systems.



Ibrahim Elshafiey received his B.S. degree in Communications and Electronics Engineering from Cairo University in 1985. He obtained his M.S. and Ph.D. degrees from Iowa State University in 1992 and 1994, respectively. He is currently working as a Professor

in the Electrical Engineering Department, King Saud University. His research interests include computational electromagnetics and biomedical imaging.



Abdulhameed Al-Sanie received his Ph.D. degree from Syracuse University, New York, in 1992. He has been with the Department of Electrical Engineering at King Saud University since 1983, where he is currently working as Department Chair. His research interests include MIMO communication systems and space time codes, Coded Modulations, and ARQ Systems.